ELSEVIER

Catalysis Today 67 (2001) 3–13

CATALYSIS TODAY

www.elsevier.com/locate/cattod

Investigation on POM reaction in a new perovskite membrane reactor

Hui Dong, Zongping Shao, Guoxing Xiong*, Jianhua Tong, Shishan Sheng, Weishen Yang

State Key Laboratory of Catalysis, Dalian Institute of Chemical Physics, Chinese Academy of Sciences, PO Box 110, Dalian 116023, PR China

Abstract

A perovskite-type oxide of $Ba_{0.5}Sr_{0.5}Co_{0.8}Fe_{0.2}O_{3-\delta}$ (BSCFO) shows mixed (electronic/oxygen ionic) conductivity at high temperatures. Membrane made of the oxide has high oxygen permeability under air/helium oxygen partial pressure gradient. At 850°C, oxygen permeation rate maintained about 1.15 ml/cm^2 min for more than 1000 h under ambient air/helium oxygen gradient. A membrane reactor constructed from the oxide membrane was applied for the partial oxidation of methane (POM) to syngas, $LiLaNiO_x/\gamma$-Al_2O_3 with 10 wt.% Ni loading was used as the packed catalyst. At the initial stage, oxygen permeation rate, methane conversion and CO selectivity were closely related with the state of the catalyst. Less than 21 h was needed for the oxygen permeation rate to reach its steady state. A membrane reactor made of BSCFO was successfully operated for POM reaction at 875°C for about 500 h without failure, with methane conversion of >97%, CO selectivity of >95% and oxygen permeation rate of about 11.5 ml/cm^2 min. Under membrane reaction condition, the POM reaction mechanism was suggested to obey the CRR (complete combustion of CH_4 to CO_2 and H_2O and a subsequent reforming reaction of the residual CH_4 and with CO_2 and H_2O to CO and H_2) mechanism.

Keywords: $Ba_{0.5}Sr_{0.5}Co_{0.8}Fe_{0.2}O_{3-\delta}$; Perovskite; Membrane reactor; Partial oxidation of methane

1. Introduction

Economical uses of natural gas have attracted extensive attention all over the world [1]. As regards, the fact that the transporting cost of natural gas rapidly rises with the increasing transportation distance, a plan called gas-to-liquid (GTL) received considerable attention during the past decade, because the most economical uses of natural gas seems to convert it into value-added liquid chemical products at site of the gas source. During the past years, extensive efforts have been made on both direct and indirect conversions of methane. The direct conversion involves oxidative coupling of methane to ethylene, and the selective oxidation of methane to methanol and formaldehyde. The indirect conversion involves reforming of natural gas to syngas ($CO + H_2$) and then using syngas to produce a series of important chemical products such as liquids fuel and methanol [2]. For the direct conversion, because reaction products are more active than the starting material, reaction products are easily to be further oxidized to CO_2 and H_2O, which leads to the low selectivity of the aimed products. Till now, the direct conversion has not found application in industry yet. At present, the application of natural gas in chemical industry is mainly by indirect conversion, and natural gas to syngas is the first step of the application.

* Corresponding author. Fax: +86-411-469-4447.
E-mail address: gxxiong@ms.dicp.ac.cn (G. Xiong).

0920-5861/01/$ – see front matter
PII: S0920-5861(01)00277-2

For the production of syngas, there are several choices including partial oxidation of methane (POM), steam reforming (which has already been industrialized), and CO_2 reforming (which is at its developing stage). Steam reforming and CO_2 reforming are both strong endothermic reactions ($CH_4 + H_2O \leftrightarrow CO + 3H_2$, $\Delta H(25^\circ C) = 206.16\,kJ/mol$, $CH_4 + CO_2 \leftrightarrow 2CO + 2H_2$, $\Delta H(25^\circ C) = 247.37\,kJ/mol$). This means that the two reactions need high temperatures, which require huge investments in plant and energy supply. POM to syngas is a weak exothermic reaction, and the reaction rate is 1–2 orders of magnitudes faster than that of the reforming reaction. Furthermore, the product ratio of CO and H_2 is 1:2, which is a perfect stoichiometry for Fisher–Tropsch reaction to methanol. However, Fisher–Tropsch reaction cannot tolerate nitrogen, and pure oxygen is required. Traditionally, oxygen is produced by cryogenic distillation of air at ultra low temperature, which increases the investment in energy supply and plant. Recently, coupling the mixed-conducting membranes with POM reaction could directly use air as the oxidant for POM reaction, which makes the separation of oxygen and catalytic oxidation in one process. Furthermore, the heat produced by POM reaction sustains the temperature needed for oxygen permeation. Such coupling simplifies the process of operation, and a reduction in GTL production cost by 20–30% can be estimated [3,4].

Mixed-conducting oxygen permeable membranes represent a class of novel ceramic membranes, which exhibit both oxygen ionic and electronic conductivity. At high temperatures, oxygen ions transport through membrane from high to low oxygen pressure side via lattice oxygen vacancies (or interlattice oxygen). Simultaneously, electrons move in a reverse direction by hopping between the multivalent metal ions. Because the membrane is dense type and only oxygen ion can incorporate into the oxygen vacancies, the permselectivity of oxygen is 100%. The driving force for oxygen permeation is the oxygen partial pressure difference across the membrane. The oxygen permeation flux of the mixed-conducting membrane under the condition of bulk diffusion controlling for oxygen permeation can be described as

$$J_{O_2} = -\frac{RT}{4^2F^2L}\int_{\ln P^h_{O_2}}^{\ln P^l_{O_2}} t_{ion}t_{el}\sigma_{total}\,d[\ln P_{O_2}] \qquad (1)$$

where L is the membrane thickness, $P^l_{O_2}$ the oxygen partial pressure of the membrane surface of the lean oxygen side (reaction side or helium sweep side), $P^h_{O_2}$ the oxygen partial pressure of the membrane surface of the high oxygen partial pressure side (air side), t_{ion} the oxygen ion transference number, t_{el} the electron transference number, σ_{total} the sum of electronic conductivity and oxygen ionic conductivity. According to Eq. (1), the oxygen permeation flux will increase with the increasing oxygen partial pressure gradient across the membrane. Under POM reaction condition, one side of the membrane surface exposed to air ($P^h_{O_2} = 0.21$ atm), and the other side of the membrane exposed to synthesis gas ($P^l_{O_2}$ can be as low as 10^{-19} atm), oxygen permeation through the membrane from air side to the reaction side where the permeated oxygen is consumed up by methane to form syngas at the presence of POM catalyst. A steady oxygen permeation flux can be sustained.

For practical application in the POM to syngas, the membrane materials must be chemically and mechanically stable at the high operating temperature and under the harsh environment. Many mixed conductors with the perovskite-type structure have shown to exhibit notably high oxygen permeability. Unfortunately, most of them are unstable under methane conversion conditions, $SrCo_{0.8}Fe_{0.2}O_{3-\delta}$, e.g., shows the highest permeability in the (La, Sr)(Co, Fe)O_x series [5,6], but it was found to undergo phase transition under low oxygen pressure or low temperature and decompose under reforming condition [7–9].

In open literature, two materials, i.e., $SrCo_{0.5}FeO_{3.25-\delta}$ and $La_{0.2}Ba_{0.8}Co_{0.2}Fe_{0.8}O_{3-\delta}$, have been tried for POM membrane reactors successfully [10–14]. Stable operation was achieved, while oxygen permeation rate was only about $4\,ml/cm^2$ min under reaction condition. Bredesen and Sogge [15] have performed an economic analysis, where they compare the catalytic membrane reactor route for syngas production with traditional autothermal reforming. For economical attractiveness, they report, that an oxygen flux of $10\,ml/cm^2$ min is needed when the membrane material is about $1600\,\$/m^2$. Recently, a new mixed-conducting membrane $Ba_{0.5}Sr_{0.5}Co_{0.8}Fe_{0.2}O_{3-\delta}$ (BSCFO) was developed in our laboratory, which shows high oxygen permeability and improved stability. The membrane was also successfully applied in

POM reaction using air as the oxidant [16]. In this paper, we would have a more detailed investigation of the POM reaction in the membrane reactor using Ni-based packed catalyst. Importance was paid to the non-steady state of the reaction during the catalyst activation stage and the long-term performance of the membrane reactor. Primary results on the reaction mechanism of POM to syngas in membrane reactor were also present.

2. Experimental

BSCFO oxide powder was synthesized by a combined citrate and EDTA complexion method. The detailed information for the preparation of BSCFO was present in [17]. The as-synthesized powder was pressed into disks in a stainless steel module (17 mm in diameter) under a hydraulic pressure of $1.3–1.9 \times 10^9$ Pa. These green disks were then sintered in a SiC muffle oven under 1150°C for 5 h with a heating and cooling rate of 1 and 2°C/min, respectively. $LiLaNiO_x/\gamma\text{-}Al_2O_3$ catalyst with 10 wt.% Ni loading was prepared by impregnation method, namely impregnating appropriate amounts of $LiNO_3$, $Ni(NO_3)_2$ and $La(NO_3)_3$ on $\gamma\text{-}Al_2O_3$ supports for 24 h, dried at 120°C under open environment, then calcined in air at 550–800°C for 4 h [18].

Fig. 1 shows a sketch of the membrane reactor assembly. One side of the membrane was exposed to air, while the other side was exposed to either diluted methane in the reaction run, or helium in the permeation run. The effective area of the membrane disk exposed to methane was 1.00 cm^2. Before the reaction run, unreduced catalyst particles of $LiLaNiO_x/\gamma\text{-}Al_2O_3$ (300 mg), were packed on the top of the membrane at 850°C, and then temperature of the reactor was increased to 1040°C with 1°C/min. After kept at 1040°C for about 5 h, the temperature of reactor was decreased to 850°C at the rate of 1°C/min. Then, 50 vol.% helium diluted methane was used for the feedstock. An HP5890 A and a GC910 chromatograph were used for analyzing the compositions of the outlet gas. A molecular sieve 5 Å was used for the separation of N_2 and O_2. A TDX-01 column was used for the separation of CO_2, CO, H_2 and CH_4. Methane conversion, CO selectivity, CO_2 selectivity and oxygen permeation flux were defined as follows:

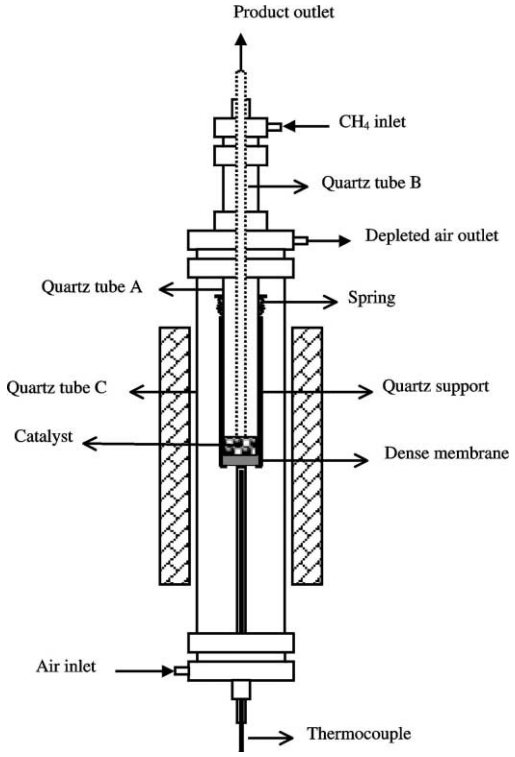

Fig. 1. Configuration of membrane reactor for POM to syngas.

$$\mathrm{CH_4\ (conversion)} = \frac{2(F_{C_2H_4} + F_{C_2H_6}) + F_{CO_2} + F_{CO}}{2(F_{C_2H_4} + F_{C_2H_6}) + F_{CO_2} + F_{CO} + F_{CH_4\ \mathrm{outlet}}} \quad (2)$$

$$\mathrm{CO\ (selectivity)} = \frac{F_{CO}}{F_{CO} + F_{CO_2} + 2(F_{C_2H_4} + F_{C_2H_6})} \quad (3)$$

$$\mathrm{CO_2\ (selectivity)} = \frac{F_{CO_2}}{F_{CO} + F_{CO_2} + 2(F_{C_2H_4} + F_{C_2H_6})} \quad (4)$$

$$J_{O_2} = \frac{F_{CO} + 2F_{CO_2} + F_{H_2O} + 2F_{O_2}(\mathrm{unreacted})}{2S} \quad (5)$$

where S is the effective membrane surface of the reaction side. The carbon balance is defined as

$$\text{Carbon balance} = \frac{F_{CH_4\,\text{outlet}} + 2(F_{C_2H_4} + F_{C_2H_6}) + F_{CO_2} + F_{CO}}{F_{CH_4\,\text{inlet}}} \quad (6)$$

The carbon balance was within a level of $100 \pm 5\%$. The deviation of carbon balance from 100% was due to the GC error and possible methane leakage from inner tube (reaction side) to outer tube (air side). There was almost no carbon deposition on the catalyst after reaction, so the carbon deposition was not included in the calculation of CO, CO_2 selectivity and methane conversion.

After the reaction performance, the temperature of reactor was rapidly decreased to room temperature. The X-ray diffraction technique was used to examine the catalyst. XRD characterization was performed with a Riguku D/Max-RB X-ray diffractometer using a copper target at 40 kV × 100 mA and scanning speed of 8°/min.

3. Results and discussion

The oxygen permeation rate of BSCFO membrane under the oxygen gradient of flowing air/helium was investigated. The temperature dependence of oxygen permeation rate through BSCFO and other membranes is shown in Fig. 2. Helium sweep rate was maintained at 30 ml/min and air feed rate was kept at 100 ml/min. Very high oxygen permeation rate was observed for the BSCFO membrane, and the permeation rate increased with the increase of temperature. Under the oxygen permeation measurement, the oxygen partial pressure of the feed side is 0.21 atm, and the oxygen partial pressure of the helium sweep side is about 0.036 atm at 850°C. Modest higher permeation was found for BSCFO than that for other membranes under similar conditions [19,20], which might be due to the higher free oxygen vacancies in BSCFO lattice than that in others.

As an ideal ceramic oxygen permeation membrane, it is not enough to possess high permeability only, but also should possess stable long-term oxygen permeation rate. Fig. 3 shows the long-term oxygen permeation stability of the BSCFO membrane at 850°C, ambient air was used as the feed gas. The permeation rate was really stable at 850°C, during more than 1000 h operation the oxygen permeation rate was not decayed, which demonstrated the stable phase structure of the BSCFO membrane at 850°C. At lower temperatures, however, the oxygen permeation flux was found to decrease very slowly with time. So in later POM investigation in the membrane reactor, the operation temperatures of the membrane were usually not lower than 850°C.

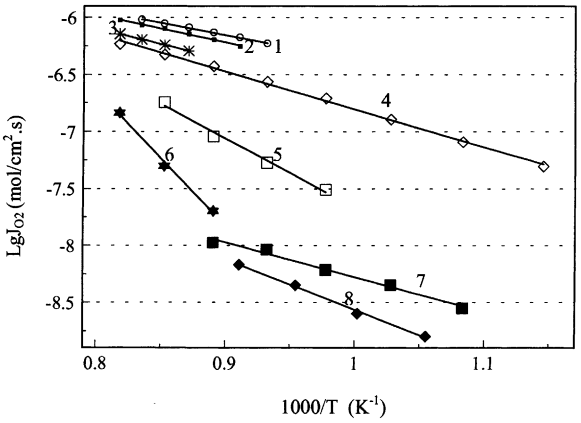

Fig. 2. Temperature dependence of oxygen permeation flux of various membranes under air/He oxygen gradient: (1) $Ba_{0.5}Sr_{0.5}Co_{0.8}Fe_{0.2}O_{3-\delta}$ ($L = 1.8$ mm) [17]; (2) $SrCo_{0.8}Fe_{0.2}O_{3-\delta}$ ($L = 1.50$ mm) [17]; (3) $BaBi_{0.3}Co_{0.2}Fe_{0.5}O_{3-\delta}$ ($L = 1.50$ mm) [19]; (4) $La_{0.3}Ba_{0.7}Co_{0.8}Fe_{0.8}O_{3-\delta}$ ($L = 1.0$ mm) [19]; (5) $Sr_{0.7}Bi_{0.3}Co_{0.2}Fe_{0.8}O_{3-\delta}$ ($L = 1.0$ mm) [19]; (6) $Sr_{0.7}Bi_{0.3}FeO_{3-\delta}$ ($L = 1.0$ mm) [20]; (7) $Y_{0.75}Bi_{0.5}Cu_{0.75}$ ($L = 2.0$ mm) [19]; (8) Er_2O_3–Bi_2O_3 ($L = 0.79$ mm) [19].

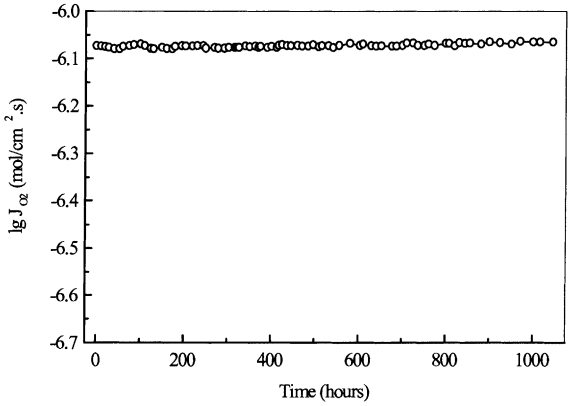

Fig. 3. Time dependence of oxygen permeation flux of $Ba_{0.5}Sr_{0.5}Co_{0.8}Fe_{0.2}O_{3-\delta}$ membrane: membrane thickness, $L = 1.46$ mm; temperature, 850°C; ambient air/helium (30 ml/min) oxygen partial pressure gradient.

The BSCFO membrane was adopted for construction of membrane reactor for POM study, since it had the high steady-state oxygen permeation rate at high temperatures. Experiments were performed on a reactor as shown in Fig. 1, where one side of the membrane disk was exposed to 50 vol.% helium diluted methane, and the other side was exposed to air (100–300 ml/min). After the methane was switched on, it was found that the only species in the eluted gas from the reaction chamber were CO, CO_2, H_2O, H_2 and unreacted CH_4, not any C_2H_4, C_2H_6 were detected. Because no gas oxygen was detected on the eluted gas, it indicated that all the oxygen permeated was consumed by the methane. It is different from that when no packed catalyst was used (the membrane surface acted as catalyst), in that case the main carbon-contained products were ethylene and ethane and considerable amount of oxygen was detected in the eluted gas [21].

Because the catalyst adopted is in the oxidation state ($NiAl_2O_4$), and the active Ni species for POM to syngas is Ni^0 (or NiO for methane combustion in the first step), so an activation stage of the catalyst is needed. However, the activation process of the catalyst would be much different in the membrane reactor from that in the packed bed reactor. In the membrane reactor, the methane to oxygen ratio is varied with the state of the catalyst, owing to the oxygen permeation flux of the membrane reactor is determined by the oxygen partial pressure gradient across the membrane, while in the fixed bed reactor the methane to oxygen ratio is constant with time (unless we adjust it on purpose). The oxygen partial pressure near the membrane surface, which determined the oxygen permeation flux of the membrane, is determined by the degree of consumption up of the oxygen permeated by the reaction near the membrane. So the initiation stage of the catalyst would be very interesting.

The time dependence of oxygen permeation rate and the catalytic performance of the BSCFO membrane during the catalyst initiation stage were shown in Fig. 4. Methane (helium diluted) flow rate were kept constant at 35 ml/min and air feed rate was 300 ml/min. At the beginning, the oxygen permeation rate ($t = 1.2$ h, $J_{O_2} = 1.78\,ml/cm^2\,min$) was only modestly higher than that under air/helium oxygen partial pressure gradient ($J_{O_2} = 1.15\,ml/cm^2\,min$). The main carbon-contained products were CO_2 (~80%) and CO (~20%); the methane conversion was low (<10%). At the first 7 h, the oxygen permeation rate increased only slowly ($t = 7.3$ h, $J_{O_2} = 2.2\,ml/cm^2\,min$), but the CO selectivity improved very quickly, at $t = 7.0$ h nearly 100% CO selectivity was achieved. The first acceleration of methane conversion has also occurred in this stage accompanied with an increasing flow rate of tail gas (the tail gas is the sum of unreacted methane, produced CO, H_2, CO_2 and the diluting gas of helium).

The above phenomena can be explained by the action of the catalyst. In the fresh catalyst used in

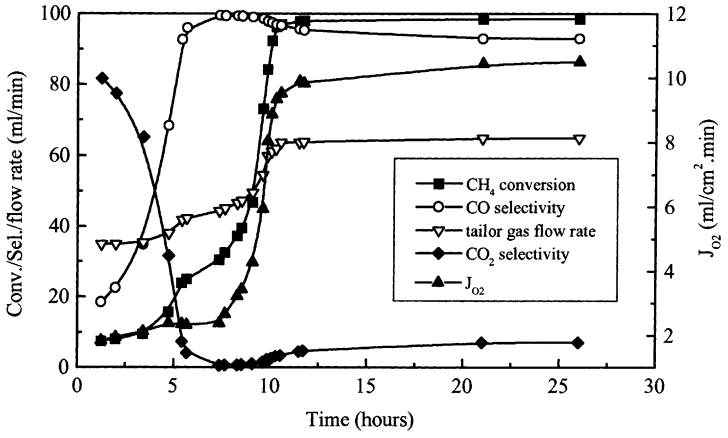

Fig. 4. Time dependence of methane conversion, CO selectivity, CO_2 selectivity tail gas flow rate and oxygen permeation flux at the catalyst activation stage at 850°C: air feed rate, 300 ml/min; 50% helium diluted methane flow rate, 35 ml/min.

this study, the nickel was in the oxidation state, i.e., $NiAl_2O_4$, which was active for methane combustion, however, the activity is very weak. The initial reduction of $NiAl_2O_4$ to Ni^0 was somewhat difficult for the reducibility of methane is relatively weak, but once some Ni^0 was appeared, the reduction process was accelerated by the produced H_2 and CO, which are highly reductive. The reduction of $NiAl_2O_4$ was first occurred at the top layer of the catalytic bed and then downward membrane surface. At the early stage of the reduction, the actual oxygen partial pressure near the membrane surface of the reaction side was little affected by the produced syngas, because there was somewhat distance between the active layer of the membrane surface and the produced syngas is less likely to reach the membrane surface, and the catalytic activity of $NiAl_2O_4$ very weak, lot of oxygen permeated is not consumed up near the membrane surface, so the oxygen partial gradient across the membrane, which determined the oxygen permeation rate, increased just modestly. With the downward movement of the active layer, the catalytic activity of the catalyst is improved, so more oxygen was consumed up near the membrane surface, the oxygen partial pressure on the reaction side decreased, and the oxygen permeation rate increased. Within the time of 8–10 h, the CH_4 conversion rocketed from about 40% to around 97% accompanied with a sharp increase in the oxygen permeation rate. The flow rate of tail gas also increased due to the sharp increase in CO and H_2 production. The CO selectivity decreased from 99.0% at $t = 7.3$ h to about 95% at $t = 12$ h. The sharp increase in the oxygen permeation was owing to the fact that, with the reach of the active layer near the membrane surface of the reaction side, the oxygen partial pressure near the membrane became very low (the oxygen partial pressure of syngas atmosphere can be as low as 10^{-19} atm). The increase in oxygen permeation rate led to the sharp increase in methane conversion. After 12 h, the increase in the oxygen permeation rate became slow down again and leveled off after 21 h. At last, 98.5% CH_4 conversion, 93.0% CO selectivity and 10.45 ml/cm^2 min oxygen permeation rate were achieved. The oxygen permeation rate was higher than that of $SrCo_{0.5}FeO_{3.25}$ membrane (4 ml/cm^2 min at 900°C) [3] and $La_{0.2}Ba_{0.8}Co_{0.2}Fe_{0.8}O_{3-\delta}$ membrane [10] (4 ml/cm^2 min at 850°C) also under POM reaction condition. Tsai et al. [10,11] operated a dense disk-shape $La_{0.2}Ba_{0.8}Co_{0.2}Fe_{0.8}O_{3-\delta}$ membrane reactor for POM using 5% Ni/Al_2O_3 as the catalyst, our two configurations of the membrane reactors are similar. For their membrane reactor, it was found that the oxygen permeation rate increased very slowly, actually a time as long as 500 h was needed for the oxygen permeation rate to reach its steady state, which was fivefold of the original one. It might demonstrate that the BSCFO membrane was more easily adjusted to the new environment than that of $La_{0.2}Ba_{0.8}Co_{0.2}Fe_{0.8}O_{3-\delta}$ membrane.

Fig. 5 shows the temperature dependence of methane conversion, CO selectivity and oxygen permeation rate with the diluted methane at the flow rate of 42.8 ml/min. Air feed rate was kept at 200 ml/min. The oxygen permeation rate and the methane conversion increased with the increasing temperature and the CO selectivity decreased on the contrary. The increase of oxygen permeation rate was due to the increase in oxygen diffusion and the surface exchange kinetics with the increasing temperature. For the excess feed of methane, the methane conversion efficiency was mainly controlled by the oxygen permeation rate, the increase in oxygen permeation rate spontaneously led to the increase in methane conversion. But the oxygen permeation rate increased slowly when the temperature was higher than 875°C, when the air feed rate was increased to 300 ml/min, the oxygen permeation rate increased obviously with temperature again (Fig. 6). It demonstrated that the oxygen permeation flux could be influenced by the air feed rate.

Fig. 7 shows the influence of air feed rates on methane conversion, CO selectivity and oxygen permeation rate at 850°C with diluted methane flow rate at 42.8 ml/min. It shows that, when the air feed rate increased from 100 to 200 ml/min the oxygen permeation rate increased, when the air flow rate was higher, i.e., 200 ml/min, its influence on the methane conversion, CO selectivity and oxygen permeation rate is negligible. It manifested that the exchanging of oxygen on the membrane surface of the rich oxygen side was not the controlling step of oxygen permeation with air flow rate >200 ml/min at 850°C. Similar experiment demonstrated that, when the air flow rate was higher than 300 ml/min, the influence of air flow rate on the oxygen permeation rate of the membrane reactor at a temperature lower than 950°C is negligible. So for the later examination, the air

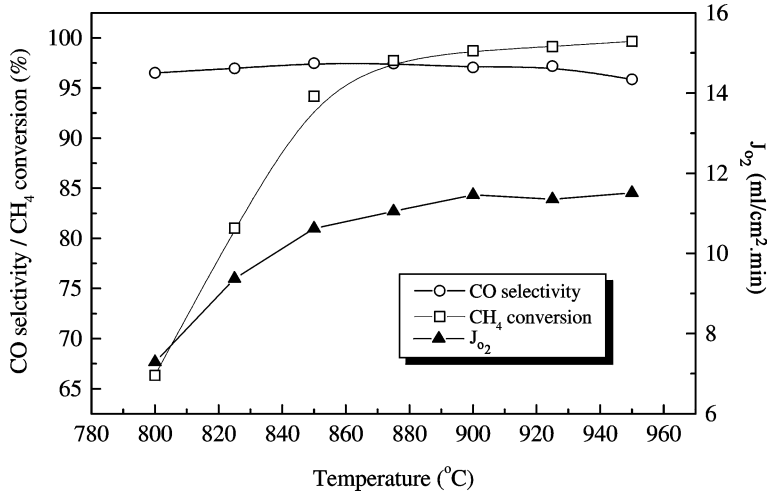

Fig. 5. Temperature dependence of methane conversion, CO selectivity and oxygen permeation rate at the air feed rate: 200 ml/min, 50% helium diluted methane flow rate: 42.8 ml/min.

flow rate was kept constant at 300 ml/min when the operation temperature was higher than 850°C.

Influence of methane flow rate on catalytic activity, selectivity and oxygen permeation flux at 850°C on a 1.48 mm thick BSCFO membrane in the reactor is showed in Fig. 8. Air feed rate was 200 ml/min. Oxygen permeation rate was kept constant when methane flow rate decreased from 42.7 to 28.5 ml/min, but as methane flow rate further decreased to 19.4 ml/min, oxygen permeation decreased with decreasing methane flow rate. According to the above phenomenon, the methane conversion mechanism in membrane reactor is likely CRR mechanism — all the oxygen is used up for the complete combustion of part of the methane, and subsequently the residual methane is reformed by steam and CO_2 to form syngas. We know that the oxygen permeation rate is determined by the oxygen gradient across the

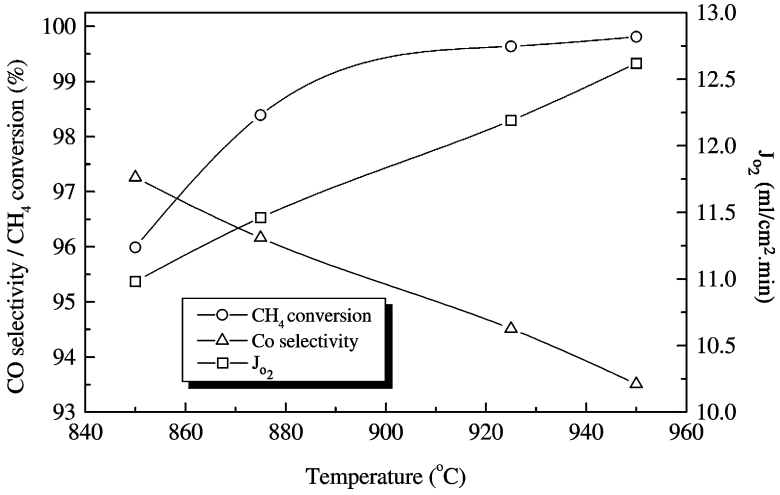

Fig. 6. Temperature dependence of methane conversion, CO selectivity and oxygen permeation rate at the air flow rate of 300 ml/min, 50% helium diluted methane flow rate: 42.8 ml/min.

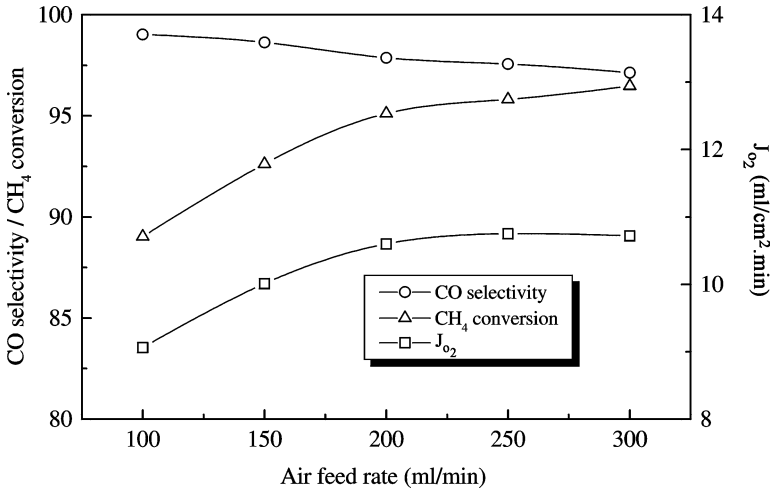

Fig. 7. Influence of air feed rate at the high oxygen partial pressure membrane side on the methane conversion, CO selectivity and oxygen permeation rate at 850°C, 50% helium diluted methane at a constant flow rate of 42.8 ml/min.

membrane. If the reaction can proceed directly to yield CO and H_2, i.e., methane reacted with oxygen to form syngas is the first step, and then the residual oxygen reacted with CO to produce CO_2 near the top of catalyst in the membrane reactor, oxygen partial pressure near the membrane surface would increase with decreasing methane flow rate, because the residual oxygen near the membrane surface would increase with decreasing methane flow rate. So under direct partial oxidation mechanism, the oxygen permeation flux would decrease with decreasing methane flow rate. However, this phenomenon did not occur in the real experiment. The reason that oxygen permeation rate decreased with decreasing methane flow rate when diluted methane flow rate is lower than 19.4 ml/min is explained as follows. Not all the introduced methane reached the membrane surface before entering the outlet tube, some methane directly enter the outlet tube because the outlet tube had some distance to the membrane surface (refer to Fig. 1).

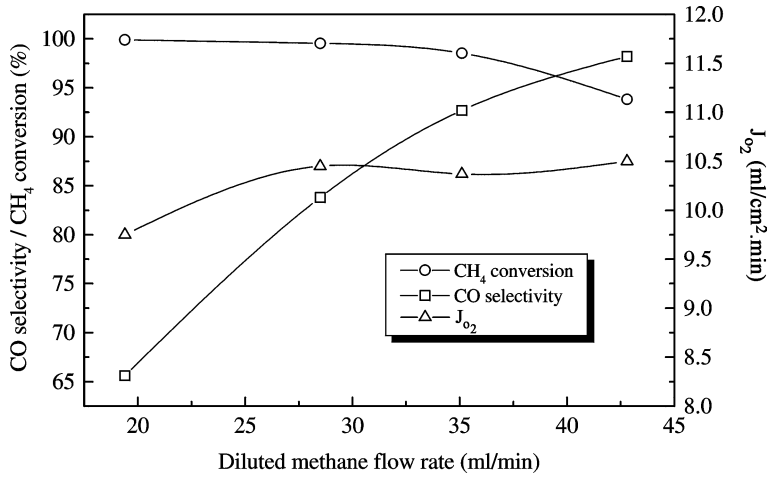

Fig. 8. Influence of methane flow rate on the methane conversion, CO selectivity and the oxygen permeation flux of the membrane at 850°C, air feed rate: 200 ml/min.

At the condition that the oxygen permeation rate was 10.5 ml/cm^2 min, and the membrane surface was 1 cm^2, at least 5.25 ml/min of methane should reach the membrane surface to consume up the permeated oxygen. Otherwise, some of the oxygen permeated could not be consumed, which led to the increased partial oxygen pressure of the membrane surface of the reaction side, and resulted in the decrease of oxygen permeation rate of the membrane reactor. It indicates that when the diluted methane flow rate was less than 19.4 ml/min (methane feed rate, 9.7 ml/min), the methane reached the membrane surface of the reaction side was likely less than 5.25 ml/min.

After the POM experiment, the air was replaced by nitrogen to sweep the membrane surface of the feed side, and in the reaction side, the methane was switched off and helium was switched on, the membrane reactor was rapidly cooled down to room temperature under the protection of helium. It was found that the catalyst showed three layers. The layer contacted with the membrane surface took the color of blue, this layer was very thin; the middle layer was gray and the third layer was black. The gray layer and black layer were divided carefully by hand, and they were later measured by XRD, respectively. Fig. 9 shows the X-ray diffraction pattern of the gray and black catalysts. NiO phase was found in the gray catalyst, however, Ni^0 phase was observed in the black catalyst. This result is the same to that of Lunsford's observation in a fixed bed reactor [22], demonstrated a CRR mechanism of the reaction, i.e., in the membrane reactor, part of methane combusted with all oxygen near the membrane surface, and subsequently the residual methane was reformed by steam and CO_2. Due to the fact that only part of methane reached the membrane surface, near the membrane surface of the reaction side the methane was in an oxygen-rich atmosphere. It was found that the surface state of the Ni-based catalyst plays a crucial role in the reaction mechanism of the POM process [23]. Under the oxygen-rich environment, methane partial oxidation favors CRR mechanism, because the catalyst surface near the membrane surface favored the oxidation state. It should be pointed out that Kikuchi and Chen [24] considered the same CRR mechanism for the methane partial oxidation in a dense palladium membrane reactor. The difference between our two reactors is that, they use dense palladium membrane to remove partial of produced hydrogen in order to modify of the CO to hydrogen ratio and to increase the conversion of methane, and we use dense oxygen membrane in order to directly use air as oxidant to reduce capital cost of operation.

For practical application, POM reaction need long-time continuous operation, so long-term stability of membrane reactor is important. It should be pointed out that the stable performance of POM reaction in the membrane reactor was determined not only by the

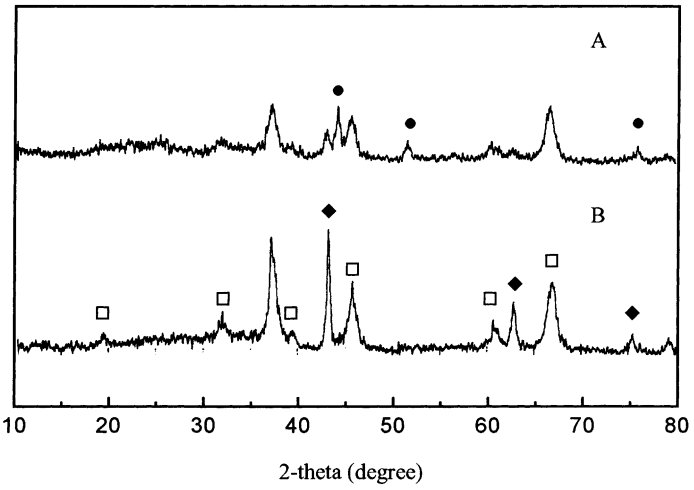

Fig. 9. XRD of the black (A) and gray (B) catalysts after operation in the membrane reactor: (□) γ-Al_2O_3; (◆) NiO; (●) Ni.

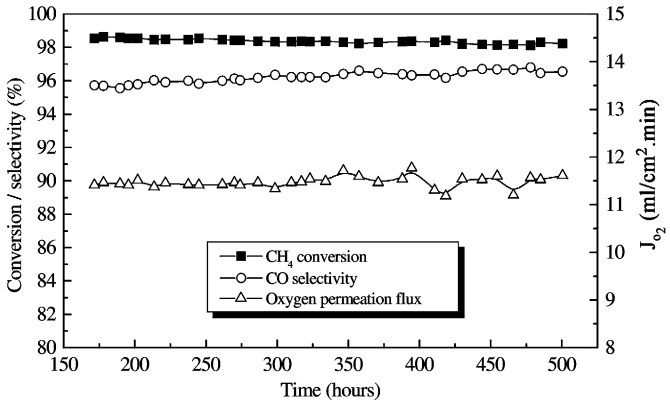

Fig. 10. Long-term membrane performance for POM to syngas at 875°C: air flow rate, 300 ml/min; 50% diluted methane flow rate, 42.8 ml/min.

stability of the membrane reactor, but also by the stability of the catalyst used. The deactivation of catalyst or the decay of membrane reactor, both could lead to the failure of the POM reaction in the membrane reactor. Our recent results of $LiLaNiO_x/\gamma\text{-}Al_2O_3$ catalyst from packed bed reactor demonstrated that it was stably operated for POM reaction for 500 h without obviously deactivation [25]. A 500 h long-term POM reaction in the membrane reactor was performed at 875°C with the diluted methane at the flow rate of 42.8 ml/min. Air feed rate was kept constant at 300 ml/min. The time dependence of CH_4 conversion, CO selectivity and oxygen permeation rate is shown in Fig. 10. Methane conversion of 97–98%, CO selectivity of 95–97% and oxygen permeation rate of around 11.2–11.8 ml/cm^2 min were achieved. During the 500 h run, the oxygen permeation was fairly stable with a value of about 11.5 ml/cm^2 min, demonstrated the excellent performance of the BSCFO membrane reactor. To investigate a longer time (>500 h) stability of the membrane reactor for POM, the stability of the catalyst should be tested first, however the data is still lacking in our laboratory for the catalyst.

4. Conclusion

BSCFO oxide has been synthesized by a combined and EDTA complexion method. Dense membrane reactor was constructed. Very high oxygen permeability was observed for BSCFO membrane, at 850°C under the gradient of air/He, J_{O_2} maintained about 1.1 ml/cm^2 min during 1000 h of operation under ambient air/helium oxygen gradient. XRD measurement shows the bulk structure of membrane still kept perovskite-type after 1000 h operation. The membrane reactor was tested for POM reaction with the presence of a reforming catalyst, $LiLaNiO_x/\gamma\text{-}Al_2O_3$. At the beginning of the reaction, reaction products were controlled by the state of the catalyst. Air feed rate could influence oxygen permeation rate when it was relatively low. The mechanism of methane conversion is likely CRR mechanism in the membrane reactor. The membrane reactor was successfully operated at 875°C for more than 500 h for POM reaction with methane conversion >97%, CO selectivity >95% and oxygen permeation rate of about 11.5 ml/cm^2 min.

Acknowledgements

The authors gratefully acknowledge financial supports from the National Natural Science Foundation of China (Grant No. 59789201), the National Advanced Materials Committee of China (Grant No. 715-006-0122) and the ministry of Science and Technology, PR China.

References

[1] G.J. Hutchings, M.S. Scurrell, J.R. Woodhouse, Chem. Soc. Rev. 18 (1989) 251.
[2] G. Henrici-Olive, S. Olive, Angew. Chem. Int. Ed. Engl. 15 (1976) 136.

[3] C.A. Udovich, Stud. Surf. Sci. Catal. 119 (1998) 417.
[4] E.P. Foster, P.J.A. Tijm, D.L. Bennett, Stud. Surf. Sci. Catal. 119 (1998) 867.
[5] Y. Teraoka, H.M. Zhang, S. Furukawa, N. Yamazoe, Chem. Lett. (1985) 1743.
[6] Y. Teraoka, T. Nobunaga, N. Yamazoe, Chem. Lett. (1988) 503.
[7] H. Kruidhof, H.J.M. Bouwmeester, R.H.E.V. Doorn, A.J. Burggraaf, Solid State Ionics 63–65 (1993) 816.
[8] L. Qiu, T.H. Lee, L.M. Liu, Y.L. Yang, A.J. Jacobson, Solid State Ionics 76 (1995) 321.
[9] S. Pei, M.S. Kleefisch, T.P. Kobylinski, J. Faber, C.A. Udovich, V. Zhang-McCoy, B. Dabrowski, U. Balachandran, R.L. Mieville, R.B. Poeppel, Catal. Lett. 30 (1995) 201.
[10] C. Tsai, A.G. Dixon, W.R. Moser, Y.H. Ma, AIChE J. 43 (1997) 2741.
[11] C. Tsai, A.G. Dixon, Y.H. Ma, W.R. Moser, M. Pascucci, J. Am. Ceram. Soc. 81 (1998) 1437.
[12] U. Balachandran, J.T. Dusek, R.L. Mieville, R.B. Poeppel, M.S. Kleefisch, S. Pei, T.P. Kobylinski, C.A. Udovich, A.C. Bose, Appl. Catal. A 133 (1995) 19.
[13] U. Balachandran, J.T. Dusek, P.S. Maiya, B. Ma, R.L. Mieville, M.S. Kleefisch, C.A. Udovich, Catal. Today 36 (1997) 265.
[14] U. Balachandran, J.T. Dusek, S.M. Sweeney, R.B. Poeppel, R.L. Mieville, P.S. Mayia, M.S. Kleefish, S. Pei, T.P. Kobylinski, C.A. Udovich, A. Bose, Am. Ceram. Soc. Bull. 74 (1995) 71.
[15] R. Bredesen, J. Sogge, Paper Presented at The United Nations Economic Commission for Europe Seminar on Ecological Applications of Innovative Membrane Technology in Chemical Industry, Chem/Sem. 21/R.12, Cetaro, Calabria, Italy, May 1–4, 1996.
[16] H. Dong, G.X. Xiong, Z.P. Shao, S.L. Liu, W.S. Yang, Chin. Sci. Bull. 45 (2000) 224.
[17] Z.P. Shao, G.X. Xiong, Y. Cong, H. Dong, J.H. Tong, W.S. Yang, J. Membr. Sci. 172 (2000) 177.
[18] Q. Miao, G.X. Xiong, S.S. Sheng, W. Cui, L. Xu, X.X. Guo, Appl. Catal. A 154 (1997) 17.
[19] Z.P. Shao, G.X. Xiong, Y. Cong, W.S. Yang, J. Membr. Sci. 164 (2000) 167.
[20] Z.P. Shao, G.X. Xiong, Y. Cong, S.S. Sheng, W. Yang, Sci. Chin. 43 (2000) 421.
[21] Z.P. Shao, H. Dong, G.X. Xiong, J.H. Tong, W. Yang, J. Membr. Sci. 183 (2001) 181.
[22] D. Dissanayake, M.P. Rosynek, K.C.C. Kharas, J.H. Lunsford, J. Catal. 132 (1991) 117.
[23] C. Li, C. Yu, S. Shen, Catal. Lett. 67 (2000) 139.
[24] E. Kikuchi, Y. Chen, Stud. Surf. Sci. Catal. 119 (1998) 441.
[25] S.L. Liu, G.X. Xiong, S.S. Sheng, W.S. Yang, Appl. Catal. A 198 (2000) 261.